Acta Polytechnica **59**(6):593–600, 2019
DOI:10.14311/AP.2019.59.0593

available online at https://ojs.cvut.cz/ojs/index.php/ap

OPTIMIZATION OF COMPUTATIONAL BURDEN OF THE POINT INFORMATION GAIN

Jan Urban*, Renata Rychtáriková, Petr Macháček, Dalibor Štys, Pavla Urbanová, Petr Císař

University of South Bohemia in České Budějovice, Faculty of Fisheries and Protection of Waters, South Bohemian Research Center of Aquaculture and Biodiversity of Hydrocenoses, Kompetenzzentrum MechanoBiologie in Regenerativer Medizin, Institute of Complex Systems, Zámek 136, 373 33 Nové Hrady, Czech Republic

* corresponding author: urbanj@frov.jcu.cz

Abstract. We developed a method of image preprocessing based on the information entropy, namely, on the information contribution made by each individual pixel to the whole image or to image's part (i.e., a Point Information Gain; PIG). An idea of the PIG calculation is that an image background remains informatively poor, whereas objects carry relevant information. In one calculation, this method preserves details, highlights edges, and decreases random noise. This paper describes optimization and implementation of the PIG calculation on graphical processing units (GPU) to overcome a high computational burden.

Keywords: Pixel information contribution, entropy, image analysis, computation optimization.

1. Introduction

One of the tasks in image analysis is an accurate segmentation of entities from their background. Correct finding of objects depends on plenty of factors, such as the kind of illumination, shadows, level of noise, proper focusing, overlaps of objects, and dissimilarity between an object and its background. The traditional methods, e.g., thresholding or edge detectors, are generally based on local or global characteristics of intensity histograms [1–4]. The final result of a chosen segmentation algorithm is more or less conditioned by the sufficiency of preprocessing computation that include color space transformations, denoising, or other adjustments [5–7]. The segmentation process is of a high quality if the borders of the objects of interest are sharp, clearly visible, and separated from the background.

A promising way for automation of the whole process of the selection of a sub-image of proper parameters is a usage of an equation of information entropy, which was defined by Shannon and generalized by Rényi [8]. Although the formula for the information entropy is well known for a longer time, other ways how to use it for one or two dimensional thresholding and filtering, e.g., [1–4, 9–11], still appear. The entropy also generally measures an information content. An important question is how much information is included in a data point and how the points can be distinguished from each other. This question was solved by a derivation of the variable Point Information Gain (PIG, Γ) [12–22] which evaluates an information content of a single pixel in local and global context. This variable says how much is one individual pixel important for understanding of an image or image's part. In addition, the method of the PIG preserves the details, highlights the edges, and decreases random noise in one calculation. Examples of usage of the PIG in image (pre)processing were published previously [12–22]

The computation tool for image preprocessing using the PIG method is called the Image Info Extractor Professional software (IIEP; Institute of Complex Systems, Nové Hrady). The theoretical concept and practical utilization of this kind of software was introduced previously and this paper is supplemental to [17]. The task of this paper is, using the examples of the Shannonian PIG with whole image approach and for cross neighbourhood for each pixel, to present a kind of computational optimization and the implementation of this computation on GPUs in order to achieve a higher computation performance of the IIEP software.

2. The Shannon entropy

The Shannon entropy is a special case of the Rényi entropy for $\alpha = 1$. Any discrete probability distribution $\mathbf{P} = \{p_0, p_1, ..., p_k\}$ fulfils the condition

$$p_j \geq 0; \sum_{j=1}^{k} p_j = 1. \quad (1)$$

In an intensity image, the approximation of the probability distribution is given by the histogram function that shows counts of the pixels $\Phi_{(x,y)}$ with intensity j at the position (h, w) in the image [3, 4].

More conditions are assumed when measuring the information. The information must be additive for two independent events with the probabilities of occurrence of p_1 and p_2:

$$I(p_{1,2}) = I(p_1) + I(p_2). \quad (2)$$

The information itself is dependent only on the probability distribution or, as in our case, on normalized histogram function. Eq. 2 describes a modified Cauchy's functional equation with the unique solution $I(p_1) = -K \times \log_2(p_1)$. In statistical thermodynamics, the constant K refers to the Boltzmann constant [23], in the Hartley information, $K = 1$ [24]. If different amounts of information occur with different probabilities, the total amount of information corresponds to the average of the individual information contributions weighted by the probabilities of their individual occurrences [24–26]. This leads to the definition of the Shannon information entropy as

$$\sum_j (p_j I_j);\ \mathscr{H}(\mathbf{P}) = -\sum_j p_j \log_2(p_j). \qquad (3)$$

The image histogram $\mathbf{N}$ is normalized to the total amount of pixels [27, 28] to fulfil the condition (1):

$$\begin{aligned} \mathbf{N} &= \left[\sum_{h,w} n_{0(h,w)}, \sum_{h,w} n_{1(h,w)}, \dots \sum_{h,w} n_{k(h,w)}\right]; \\ n_{j(h,w)} &= \begin{cases} 1 & \text{for} \quad \Phi_{(h,w)} = j \\ 0 & \text{for} \quad \Phi_{(h,w)} \neq j. \end{cases} \qquad (4) \\ p_{j(h,w)} &= \frac{n_{j(h,w)}}{WH}; \\ \mathbf{P} &= \left[\sum_{h,w} p_{0(h,w)}, \sum_{h,w} p_{1(h,w)}, \dots \sum_{h,w} p_{k(h,w)}\right], \end{aligned}$$

where WH is a total amount of pixels in an image of the size of $[H \times W]$. Then, the normalized histogram function P is used to define the information in the form of the Shannon entropy as

$$\mathscr{H}(\mathbf{P}) = -\sum_j p_j \log_2 p_j. \qquad (5)$$

For the simplification of the next deduction, the binary logarithm $\log_2$, which explains the information in bits, is supplied by natural algorithm ln.

3. Point Information Gain

In the form of the variable PIG ($\Gamma^{(i)}$), the Shannon entropy allows to measure an information content of either the whole image or a selected part of the image. The key idea for the definition of the PIG was if the occurrence of the intensity of a single pixel is a surprise. One can predict that, on the one hand, the background pixels will not carry much information and, on the other hand, the pixels of structurally complicated objects will increase the entropy on their positions after discarding one of them. In order to investigate the contribution of one single pixel with intensity value i to the total entropy, it is necessary to introduce a histogram $\mathbf{N}^{(i)}$, which is created without this investigated pixel:

$$n_j^{(i)} = \begin{cases} n_j & \text{for} \quad j \neq i \\ n_j - 1 & \text{for} \quad j = i. \end{cases}$$

The intensity value i of the investigated pixel $\Phi_{(h,w)} = \Phi_{(x,y)}$ was now discarded from the computation, but only once. One single pixel of intensity j will only decrease the histogram value $n_j^{(i)}$ on its intensity position i. Then, the histogram is normalized according to condition (1). The probability (value of the normalized histogram) $p_i^{(i)}$ of the intensity i is slightly lower than the probability p_i of the primary normalized histogram $\mathbf{P}$ (with all pixels). The other probabilities $p_j^{(i)}$, where j is not the value of the investigated pixel i, are slightly higher than the probability p_j of the primary normalized histogram $\mathbf{P}$ (with all pixels). Then, the second Shannon information entropy $\mathscr{H}(\mathbf{P}^{(i)})$ without the pixel of intensity i at the position (x, y) is computed from the modified normalized histogram $P^{(i)}$ as

$$\mathscr{H}(\mathbf{P}^{(i)}) = -\sum_j p_j^{(i)} \ln(p_j^{(i)}), \qquad (6)$$

where the individual information contributions $\ln(p_j^{(i)})$ as well as their weights $p_j^{(i)}$ slightly differ from those in the Shannon information entropy $\mathscr{H}(\mathbf{P})$ (Eq. 5). Thus, using Eqs. (5)–(6), we obtained two different values of the information entropy: The entropy $\mathscr{H}(\mathbf{P})$ represents the total information in the whole original image, whereas the entropy $\mathscr{H}(\mathbf{P}^{(i)})$ represents the information in the image without the investigated pixel.

$$\Gamma^{(i)} = \mathscr{H}(\mathbf{P}) - \mathscr{H}(\mathbf{P}^{(i)}) = \mathscr{H} - \mathscr{H}^{(i)} \qquad (7)$$

refers then to a difference between the entropy of the two histograms and thus also to the difference between the entropy of two images – with and without the investigated pixel $\Phi_{(x,y)}$ of the intensity i. Recall that the histograms $\mathbf{P}$ and $\mathbf{P}^{(i)}$ were normalized and, therefore, the difference $\Gamma^{(i)}$ is usually a small number. (In the IIEP software, the Point Information Gain is defined with the opposite sign as $\Gamma^{(i)} = \mathscr{H}^{(i)} - \mathscr{H}$.) The difference $\Gamma^{(i)}$ represents either the entropy contribution of the pixel $\Phi_{(x,y)}$ or the contribution of the intensity value of the pixel $\Phi_{(x,y)}$ to the information content of the image. In other words, the transformation of the intensity value of the pixel $\Phi_{(x,y)}$ value to its contribution to the image via Eq. (7) represents the information contribution carried by this pixel. The computation of the $\Gamma^{(i)}$ for each single pixel transforms an original image into an entropy map, i.e., into an image that shows the contribution of each pixel to the total information content of the image.

The variable $\Gamma^{(i)}$ is dependent only on the intensity of the pixel $\Phi_{(x,y)}$ and does not carry any information about the pixel's position. However, the histogram can include pixels from not only the whole image but also from a selected area around an investigated pixel. If the image has a semi-uniform background with changes in intensity and the background is completely different in different parts of the image, it is

advantageous to use the row and the column with the investigated pixel in the centre as the area for the computation of the intensity histogram

$$\mathbf{N} = \mathbf{N}_{(x)} + \mathbf{N}_{(y)} - \mathbf{E}_i, \tag{8}$$

where the value of pixel $\Phi_{(x,y)}$ is counted only once. The value of the second pixel $\Phi_{(x,y)}$ is subtracted using the unit histogram $\mathbf{E}_i = [0, 0, \ldots, 1, \ldots, 0, 0]$ with 1 at the position relevant to $n_j = n_i > 0$. The outputs consist of the amount of information for the cross centred on the investigated pixel itself. The additional histogram is again a histogram of the values from the cross, however, in this case, the intensity value of the center pixel $\Phi_{(x,y)}$ was discarded:

$$\mathbf{N}^{(i)} = \mathbf{N}_{(x)} + \mathbf{N}_{(y)} - 2\mathbf{E}_i. \tag{9}$$

The subsequent application of Eq. (5) results in entropies $\mathscr{H}_{(x,y)}(P) = \mathscr{H}_{(x,y)}$ and $\mathscr{H}_{(x,y)}(P^{(i)}) = \mathscr{H}^{(i)}_{(x,y)}$ with and without the center pixel, respectively. The difference $\Gamma^{(i)}_{(x,y)} = \mathscr{H}_{(x,y)} - \mathscr{H}^{(i)}_{(x,y)}$ refers to the difference between the information content of these two crosses. Recall again that the difference $\Gamma^{(i)}_{(x,y)}$ is a small number and represents either the entropy contribution of pixel $\Phi_{(x,y)}$ or the contribution of the value of pixel $\Phi_{(x,y)}$ to the cross.

Both (whole and cross) PIG can be considered as special cases of the Kullback-Leibler divergence [29] of two distributions: one distribution is formed from the neighbourhood of the investigated pixel including this pixel, while the second distribution is formed from the same neighbourhood but without this pixel. The whole approach considers the whole image as the neighbourhood, while the cross approach considers the designed cross with the investigated pixel in the center.

Thus, the novelty of the PIG approach lies in the practical definition of the investigated normalized distributions.

4. Optimization of the algorithm

4.1. Point Information Gain for the whole image

The $\Gamma^{(i)}$ values for the whole image does not need to be computed for each pixel repeatedly. The value of the total entropy $\mathscr{H}$ remains the same through the whole image and the value of the entropy $\mathscr{H}^{(i)}$ is the same for all pixels $\Phi_{(x,y)}$ with the same intensity $j = i$. The algorithm was optimized by the modification of the relevant equations as follows:

The histogram $\mathbf{N} = [n_0, n_1, \ldots n_{2^d-1}]$ for the whole image was redefined to

$$\begin{aligned} n_j = ||\{\forall(x,y) : \Phi_{(x,y)} = j \wedge x \in \{1, 2, \ldots, H\} \\ \wedge y \in \{1, 2, \ldots, W\}\}||; \\ j = [0, 1, \ldots, i, \ldots, 2^d - 1]. \end{aligned}$$

The entropy $\mathscr{H}$ can be subsequently explained as

$$\mathscr{H} = -\sum_{j=0}^{2^d-1} p_j \ln(p_j),$$

$$\mathscr{H} = -\sum_{j=0}^{2^d-1} \frac{n_j}{WH} \ln\Big(\frac{n_j}{WH}\Big),$$

$$\mathscr{H} = -\sum_{j=0}^{2^d-1} \frac{n_j}{WH} [\ln(n_j) - \ln(WH)],$$

$$\mathscr{H} = \frac{\ln(WH)}{WH} \underbrace{\sum_{j=0}^{2^d-1} n_j}_{WH} - \frac{1}{WH} \sum_{j=0}^{2^d-1} n_j \ln(n_j),$$

$$\mathscr{H} = \ln(WH) - \frac{1}{WH} \sum_{j=0}^{2^d-1} n_j \ln(n_j). \tag{10}$$

The function $\mathscr{H}^{(i)}$ which explains the entropy of the modified image with the omitted investigated pixel $\Phi_{(x,y)}$ was reformulated as

$$\mathscr{H}^{(i)} = -\sum_{j=0}^{2^d-1} p_j^{(i)} \ln(p_j^{(i)}),$$

$$\mathscr{H}^{(i)} = -\sum_{j=0}^{2^d-1} \frac{n_j^{(i)}}{WH-1} \ln\left(\frac{n_j^{(i)}}{WH-1}\right),$$

$$\mathscr{H}^{(i)} = -\sum_{j=0}^{2^d-1} \frac{n_j^{(i)}}{WH-1} [\ln(n_j^{(i)}) - \ln(WH-1)],$$

$$\mathscr{H}^{(i)} = \frac{\ln(WH-1)}{WH-1} \underbrace{\sum_{j=0}^{2^d-1} n_j^{(i)}}_{WH-1} - \frac{\sum_{j=0}^{2^d-1} n_j^{(i)} \ln(n_j^{(i)})}{WH-1},$$

$$\mathscr{H}^{(i)} = \ln(WH-1) - \frac{\sum_{j=0}^{2^d-1} n_j^{(i)} \ln(n_j^{(i)})}{WH-1}. \tag{11}$$

The histogram $\mathbf{N}^{(i)}$ is then defined as

$$n_j^{(i)} = \begin{cases} n_j & j \neq i \\ n_j - 1 & j = i, \end{cases} \quad j = [0, 1, \ldots, 2^d - 1].$$

The first optimization was performed as

$$\begin{aligned} n^{(i)} \Leftrightarrow \mathscr{H}^{(i)} \Leftrightarrow \Phi_{(x,y)} = i; \\ x \in \{1, 2, \ldots, H\}; \\ y \in \{1, 2, \ldots, W\}; \\ i \in \{0, 1, \ldots, 2^d - 1\}. \end{aligned}$$

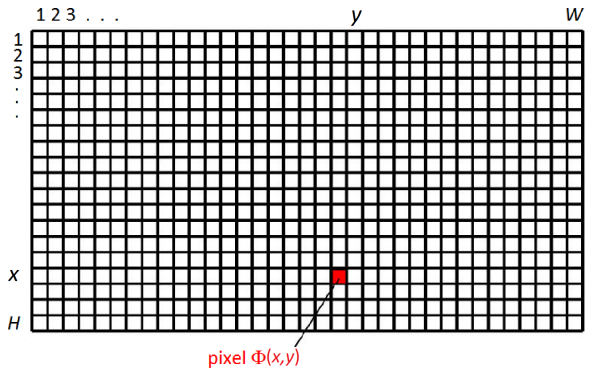

FIGURE 1. Image of the size of $[H \times W]$ with the intensity levels of d bits.

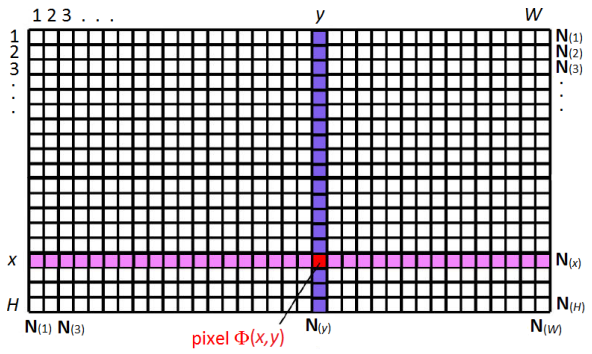

FIGURE 2. Image of the size of $[H \times W]$ with the intensity levels of d bits, with investigated cross.

From this optimization as well as Eq.(7) follows directly that the entropy $\mathscr{H}^{(i)}$ is dependent only on the intensity i of the pixel $\Phi_{(x,y)}$ and not on the pixel's position (x, y) in the image. Then, the entropy $\mathscr{H}^{(i)}$ can be redefined as

$$\mathscr{H}^{(i)} = (\mathscr{H}^{(i)} | \Phi_{(x,y)} = i); \qquad i = [0, 1, \ldots, 2^d - 1].$$

Eventually, the PIG for the whole image is subsequently explained as

$$\Gamma^{(i)} = \mathscr{H} - \mathscr{H}^{(i)},$$

$$\Gamma^{(i)} = \ln(WH) - \frac{\sum_{j=0}^{2^d-1} n_j \ln(n_j)}{WH} - \ln(WH - 1) + \frac{\sum_{j=0}^{2^d-1} n_j^{(i)} \ln(n_j^{(i)})}{WH - 1},$$

$$\Gamma^{(i)} = \ln\left(\frac{WH}{WH-1}\right) - \frac{n_i \ln(n_i) + \sum_{j=0}^{i-1} n_j \ln(n_j) + \sum_{j=i+1}^{2^d-1} n_j \ln(n_j)}{WH} + \frac{(n_i - 1)\ln(n_i - 1)}{WH - 1} + \frac{\sum_{j=0}^{i-1} n_j \ln(n_j) + \sum_{j=i+1}^{2^d-1} n_j \ln(n_j)}{WH - 1},$$

$$\Gamma^{(i)} = \ln\left(\frac{WH}{WH-1}\right) + \frac{1}{WH(WH-1)} \underbrace{\left(\sum_{j=0}^{i-1} n_j \ln(n_j) + \sum_{j=i+1}^{2^d-1} n_j \ln(n_j)\right)}_{\sum_{j=0}^{2^d-1} (n_j \ln(n_j)) - n_i \ln(n_i)} - \frac{n_i \ln(n_i)}{WH} + \frac{(n_i - 1)\ln(n_i - 1)}{WH - 1},$$

$$\Gamma^{(i)} = \ln\left(\frac{WH}{WH-1}\right) + \frac{\sum_{j=0}^{2^d-1} n_j \ln(n_j)}{WH(WH-1)} + \frac{1}{WH-1}\left[(n_i - 1)\ln(n_i - 1) - n_i \ln(n_i)\right],$$

$$\Gamma^{(i)} = \ln\left(\frac{WH}{WH-1}\right) + \frac{\sum_{j=0}^{2^d-1} n_j \ln(n_j)}{WH(WH-1)} + \frac{1}{WH-1} \ln \frac{(n_i - 1)^{(n_i - 1)}}{n_i^{(n_i)}}. \tag{12}$$

From Eq. 12 follows that the $\Gamma^{(i)}$ can be evaluated as

$$\Gamma^{(i)} = B + C \ln \frac{(n_i - 1)^{(n_i - 1)}}{n_i^{(n_i)}}, \tag{13}$$

where the constant $C = \frac{1}{WH-1}$ and the base $B = \ln\left(\frac{WH}{WH-1}\right) + \frac{1}{WH(WH-1)} \sum_{j=0}^{2^d-1} n_j \ln(n_j)$.

4.2. Point Information Gain for the cross computation

A column histogram $\mathbf{N}_{(y)}$ is defined as

$$\mathbf{N}_{(y)} = [n_{0(y)}, n_{1(y)}, \ldots, n_{(2^d-1)(y)}]; \quad y = [1, 2, \ldots, W]; \quad j = [0, 1, \ldots, i, \ldots, 2^d - 1].$$

Similarly, a row histogram $\mathbf{N}^{(x)}$ is defined as

$$\mathbf{N}_{(x)} = [n_{0(x)}, n_{1(x)}, \ldots, n_{(2^d-1)(x)}]; \quad x = [1, 2, \ldots, H]; \quad j = [0, 1, \ldots, i, \ldots, 2^d - 1].$$

The elements of the unit histogram $\mathbf{E}_i$ are (cf. Eqs. (8)–(9))

$$e_j = \begin{cases} 0 & j \neq i = \Phi_{(x,y)} \\ 1 & j = i = \Phi_{(x,y)} \end{cases} \quad j = [0, 1, \ldots, i, \ldots, 2^d - 1].$$

The entropy $\mathscr{H}_{(x,y)}$ for computation from the column histogram $\mathbf{N}^{(y)}$ and row histogram $\mathbf{N}_{(x)}$ of the cross with the center pixel on, of the intensity i at the position (x, y), can be written as

$$\mathscr{H}_{(x,y)} = -\sum_{j=0}^{2^d-1} p_j \ln(p_j),$$

$$\mathscr{H}_{(x,y)} = \\ = -\sum_{j=0}^{2^d-1} \frac{n_{j(x)} + n_{j(y)} - e_j}{H+W-1} \ln \frac{n_{j(x)} + n_{j(y)} - e_j}{H+W-1},$$

$$\mathscr{H}_{(x,y)} = \\ = \sum_{j=0}^{2^d-1} \frac{n_{j(x)} + n_{j(y)} - e_j}{H+W-1} \ln(H+W-1) \\ - \sum_{j=0}^{2^d-1} \frac{n_{j(x)} + n_{j(y)} - e_j}{H+W-1} \ln(n_{j(x)} + n_{j(y)} - e_j),$$

$$\mathscr{H}_{(x,y)} = \\ = \frac{\ln(H+W-1)}{H+W-1} \underbrace{\sum_{j=0}^{2^d-1} n_{j(x)} + n_{j(y)} - e_j}_{H+W-1} \\ - \frac{\sum_{j=0}^{2^d-1} (n_{j(x)} + n_{j(y)} - e_j) \ln(n_{j(x)} + n_{j(y)} - e_j)}{H+W-1},$$

$$\mathscr{H}_{(x,y)} = \\ = \ln(H+W-1) \\ - \frac{\sum_{j=0}^{2^d-1} (n_{j(x)} + n_{j(y)} - e_j) \ln(n_{j(x)} + n_{j(y)} - e_j)}{H+W-1},$$

$$\begin{aligned} \mathscr{H}_{(x,y)} &= \\ &= \ln(H+W-1) \\ &- \frac{\sum_{j=0}^{i-1} (n_{j(x)} + n_{j(y)}) \ln(n_{j(x)} + n_{j(y)})}{H+W-1} \\ &- \frac{\sum_{j=i+1}^{2^d-1} (n_{j(x)} + n_{j(y)}) \ln(n_{j(x)} + n_{j(y)})}{H+W-1} \\ &- \frac{(n_{i(x)} + n_{i(y)} - 1) \ln(n_{i(x)} + n_{i(y)} - 1)}{H+W-1}. \end{aligned} \tag{14}$$

Similarly, the entropy $\mathscr{H}^{(i)}_{(x,y)}$ for the computation from the column histogram $\mathbf{N}_{(y)}$ and row histogram $\mathbf{N}_{(x)}$ of the cross without center pixel, of the intensity i at the position (x, y), is

$$\mathscr{H}^{(i)}_{(x,y)} = -\sum_{j=0}^{2^d-1} p^{(i)}_j \ln(p^{(i)}_j),$$

$$\mathscr{H}^{(i)}_{(x,y)} = \\ = -\sum_{n=0}^{2^d-1} \frac{n_{j(x)} + n_{j(y)} - 2e_j}{H+W-2} \ln \frac{n_{j(x)} + n_{j(y)} - 2e_j}{H+W-2},$$

$$\mathscr{H}^{(i)}_{(x,y)} = \ln(H+W-2) \\ - \frac{\sum_{j=0}^{2^d-1} (n_{j(x)} + n_{j(y)} - 2e_j) \ln(n_{j(x)} + n_{j(y)} - 2e_j)}{H+W-2},$$

$$\begin{aligned} \mathscr{H}^{(i)}_{(x,y)} &= \\ &= \ln(H+W-2) \\ &- \frac{\sum_{j=0}^{i-1} (n_{j(x)} + n_{j(y)}) \ln(n_{j(x)} + n_{j(y)})}{H+W-2} \\ &- \frac{\sum_{j=i+1}^{2^d-1} (n_{j(x)} + n_{j(y)}) \ln(n_{j(x)} + n_{j(y)})}{H+W-2}. \end{aligned} \tag{15}$$

It gives a PIG for the cross computation as

$$\Gamma^{(i)}_{(x,y)} = \mathscr{H}_{(x,y)} - \mathscr{H}^{(i)}_{(x,y)},$$

$$\begin{aligned} \Gamma^{(i)}_{(x,y)} &= \\ &= \ln\left(\frac{H+W-1}{H+W-2}\right) \\ &+ \frac{\sum_{j=0}^{i-1} (n_{j(x)} + n_{j(y)}) \ln(n_{j(x)} + n_{j(y)})}{(H+W-1)(H+W-2)} \\ &+ \frac{\sum_{j=i+1}^{2^d-1} (n_{j(x)} + n_{j(y)}) \ln(n_{j(x)} + n_{j(y)})}{(H+W-1)(H+W-2)} \\ &- \frac{(n_{i(x)} + n_{i(y)} - 1)}{H+W-1} \ln(n_{i(x)} + n_{i(y)} - 1) \\ &+ \frac{(n_{i(x)} + n_{i(y)} - 2)}{H+W-2} \ln(n_{i(x)} + n_{i(y)} - 2). \end{aligned} \tag{16}$$

Let us introduce the vector t defined as

$$\begin{aligned} t =& [t_{(0)}, t_{(1)}, t_{(2)}, \ldots, t_{(H+W-1)}] = \\ =& [0\ln(0), 1\ln(1), 2\ln(2), \\ & \ldots, (H+W-1)\ln(H+W-1)]. \end{aligned}$$

Then, Eq. (16) can be written as

$$\begin{aligned} \Gamma^{(i)}_{(x,y)} &= \\ &= \ln\left(\frac{H+W-1}{H+W-2}\right) \\ &+ \frac{\sum_{j=0}^{i-1} t_{(n_{j(x)}+n_{j(y)})}}{(H+W-1)(H+W-2)} \\ &+ \frac{\sum_{j=i+1}^{2^d-1} t_{(n_{j(x)}+n_{j(y)})}}{(H+W-1)(H+W-2)} \\ &- \frac{t_{(n_{i(x)}+n_{i(y)}-1)}}{H+W-1} + \frac{t_{(n_{i(x)}+n_{i(y)}-2)}}{H+W-2}. \end{aligned} \tag{17}$$

In this way, the time consuming computation of the logarithms was replaced by the summing of precomputed vectors $k\ln(k)$. The length of the vector t does not depend on the number of pixels in the image but on the dimensions (sizes of the sides) of the image. The number of rows and columns of the image determines how many points in the histogram created from the cross is available. It is, however, possible that some values in the vector t will never be used in the computation. Nevertheless, due to the possibility of searching in the list of all stored $k\ln(k)$, the approach of the precomputed histograms makes the computation faster. Eq. (17) implicates

$$\begin{aligned}
\Gamma^{(i)}_{(x,y)} &= C^{(x,y)} + B^{(x,y)} + F^{(x,y)};\\
C_{(x,y)} &= \ln\left(\frac{H+W-1}{H+W-2}\right);\\
B_{(x,y)} &= \frac{\sum_{j=0}^{i-1}\left(n_{j(x)}+n_{j(y)}\right)\ln\left(n_{j(x)}+n_{j(y)}\right)}{(H+W-1)(H+W-2)}\\
&\quad + \frac{\sum_{j=i+1}^{2^d-1}\left(n_{j(x)}+n_{j(y)}\right)\ln\left(n_{j(x)}+n_{j(y)}\right)}{(H+W-1)(H+W-2)};\\
F_i &= \frac{\left(n_{i(x)}+n_{i(y)}-2\right)\ln\left(n_{i(x)}+n_{i(y)}-2\right)}{H+W-2}\\
&\quad - \frac{\left(n_{i(x)}+n_{i(y)}-1\right)\ln\left(n_{i(x)}+n_{i(y)}-1\right)}{H+W-1}.
\end{aligned} \tag{18}$$

In Eq. 18 the term $C_{(x,y)}$ is a constant, the $B_{(x,y)}$ is a base of the computation, and the F_i corresponds to a fluctuating part of the computation.

5. Implementation on GPU

The algorithm optimised above can be further split into a few threads when multi-core CPUs can be fully utilized, however this is relevant mainly for batch processing of image sets. The computation process was further optimized by an implementation on graphics cards [30]. The algorithm was executed using the CUDA architecture to run on NVIDIA hardware. The key to the next acceleration was to fit the algorithm to GPU highly-parallel architecture which is typical of a double hierarchy. All multiprocessors can access data to the device memory. In the CUDA data-parallel programming, the data has to be split into two levels of algorithmically independent parts, into a grid of blocks where a kernel processes the block with the same algorithm. During the processing of the block, several threads run – the second level of the hierarchy. All threads of one block run per one multiprocessor.

The IIEP software tries to detect the graphics card with the CUDA support and, if the card is available, the calculation is realised as the parallel computation on the graphics card kernels (GPU). Depending on the image resolution and the type of the entropy calculation, the calculation is typically 50–150× faster on the GPU than on the CPU. The original concept of the software expected an 8-bpc (bits per channel) images (which could be optimized directly for the GPU memory block), while the current cameras are also able to provide raw file formats with ≥10 bpc (which requires a different GPU static-field allocation). The possibility to work with the raw data files deals with signal processing without debayerization [14].

6. Conclusion

We investigated the degree of modality for a computation of the difference of two entropies: $\mathscr{H}$, entropy with a central pixel $\Phi_{(x,y)}$, and $\mathscr{H}^{(i)}$, entropy without such pixel. An output image then represents a map of pixels' importance. We simplified the calculation of the information contribution of a pixel to the whole Shannonian information of the image and to local information explained for pixels lying on shanks crossing the studied pixel $\Phi_{(x,y)}$. The pre-computation of a fixed set (for a given bit precision) of possible logarithm values reduces the total number of necessary calculations in the algorithm and decrease the computational burden in the evaluation of the entropy difference. The calculation kernel was implemented for hardware acceleration using a graphics card.

List of symbols

B Base in computation of $\Gamma^{(i)}$

$B_{(x,y)}$ Base in computation of $\Gamma^{(i)}_{(x,y)}$

C Constant member in computation of $\Gamma^{(i)}$

$C_{(x,y)}$ Constant member in computation of $\Gamma^{(i)}_{(x,y)}$

CUDA Compute Unified Device Architecture

d Image intensity bit depth

e_j Element of the unit vector $\mathbf{E}_i$

$\mathbf{E}_i$ Unit vector [0,0, ...,1,...,0,0], where 1 is at the position e_i

F_i Fluctuating in computation of $\Gamma^{(i)}_{(x,y)}$

GPU Graphical Processing Unit

h Row position of the pixel of intensity j

H Image height (in pixels)

$\mathscr{H}(\mathbf{P}) = \mathscr{H}$ Shannon entropy for probability histogram function of the whole image

$\mathscr{H}_{(x,y)}$ Shannon entropy for probability histogram function from the cross around an investigated pixel of the intensity i at the position (x, y)

$\mathscr{H}(\mathbf{P}^{(i)}) = \mathscr{H}^{(i)}$ Shannon entropy for probability histogram function from the whole image without an investigated pixel of intensity i

$\mathscr{H}^{(i)}_{(x,y)}$ Shannon entropy for probability histogram function from the cross around and without an investigated pixel of the intensity i at the position (x, y)

i Intensity of an investigated pixel

I Information

IIEP Image Info Extractor Professional software

j Pixel intensity; $j \in \{0, 1, \ldots, i, \ldots, i, \ldots, k\}$

K Weight of the entropic contribution; e.g., $K = 1$ in the Hartley and Shannon entropy; $K = 1.38 \times 10^{-23}$ in the Boltzmann entropy

$n_{j(h,w)} = n_j$ Contribution of the pixel of intensity j at the position (h, w) to the histogram $\mathbf{N}$

$n_j^{(i)}$ Element in the histogram $\mathbf{N}$, where a pixel of intensity i is discarded

$n_{j(x)}$ Element of the intensity histogram of an image pixel row x

$n_{j(y)}$ Element of the intensity histogram of an image pixel column y

$\mathbf{N}$ Image histogram function

$\mathbf{N}^{(i)}$ Intensity histogram without an investigated pixel of intensity i

$\mathbf{N}_{(x)}$ Intensity histogram for the image pixel row x

$\mathbf{N}_{(y)}$ Intensity histogram for the image pixel column y

p_i Probability of the occurrence of the investigated pixels of intensity i in histogram $\mathbf{P}$

$p_{j(h,w)} = p_j$ Contribution of the pixel of intensity j at the position (h, w) to the probability histogram $\mathbf{P}$;

$p_j^{(i)}$ Element in the probability histogram $\mathbf{P}$, where the pixel of intensity i is discarded

$\mathbf{P}$ Discrete probability distribution (of the whole image)

$\mathbf{P}^{(i)}$ Probability intensity histogram without an investigated pixel of the intensity i

PIG Point Information Gain; Γ

t Mathematical substitution for a vector of weighted logarithms with element $t_{(n_j)} = n_j \ln n_j$

$t_{(n_j)}$ Element of the vector t of weighted logarithms

w Column position of the pixel of intensity j

W Image width (in pixels)

x Row position of the pixel of intensity i

y Column position of the pixel of intensity i

α Rényi dimensionless coefficient

$\Gamma^{(i)}$ Point Information Gain for a pixel of intensity i (from a whole-image histogram)

$\Gamma^{(i)}_{(x,y)}$ Point Information Gain for a pixel of intensity i from a histogram from pixels forming a cross around the investigated pixel

$\Phi_{(h,w)}$ Pixel of intensity j at the position (h, w)

$\Phi_{(x,y)}$ Pixel (of) intensity i at the position (x, y)

Acknowledgements

Authors are thankful to J. Vaněk, T. Levitner, A. Zhyrova, and V. Březina for several discussions. This work was supported by the Ministry of Education, Youth and Sports of the Czech Republic—projects CENAKVA (LM2018099) and the CENAKVA Centre Development (No. CZ.1.05/2.1.00/19.0380)—and from the European Regional Development Fund in frame of the project Kompetenzzentrum MechanoBiologie (ATCZ133) in the Interreg V-A Austria–Czech Republic programme. The work was further financed by the TA CR Gama PoC 03-24-Rychtáriková sub-project.

References

[1] S. Beucher. Applications of mathematical morphology in material sciences: A review of recent developments. international metallography conference, colmar, france. *Proc MC95* pp. 41–46, 1945.

[2] N. Otsu. A threshold selection method from gray-level histogram. *IEEE Trans Syst Man Cybern* **9**(1):62–66, 1979. DOI:10.1109/TSMC.1979.4310076.

[3] M. Sonka, V. Hlavac, R. Boyle. *Image processing, analysis and machine vision*. Brooks/Cole Publishing Company, 1999.

[4] R. C. Gonzales, R. E. Woods. *Digital image processing*. Addison-Wesley Publishing Co., Reading, Mass.-London-Don Mills, Ont, 1992.

[5] J. Yang, W. Lu, A. Waibel. Skin-color modeling and adaptation. Proc. ACCV 1998-Vol. II. *Lect Notes Comp Sci* **1352**:687–694, 1998. DOI:10.1007/3-540-63931-4_278.

[6] L. Vincent. Morphological grayscale reconstruction in image analysis: applications and efficient algorithms. *IEEE Trans Image Process* **2**(2):176–201, 1993. DOI:10.1109/83.217222.

[7] J. Vaněk, J. Urban, Z. Gardian. Automated detection of photosystems II in electron microscope photographs. Technical Computing Prague, Prague, Czechia pp. 102–105, 2006.

[8] A. Rényi. On measures of information and entropy. *Proc 4th Berkeley Symp Math Stat Prob* **1**:547–561, 1961.

[9] R. Moddemeijer. On estimation of entropy and mutual information of continuous distributions. *Signal Process* **16**(3):233–246, 1989. DOI:10.1016/0165-1684(89)90132-1.

[10] T. Pun. A new method for grey-level picture thresholding using the entropy of the histogram. *Signal Process* **2**(3):223–237, 1980. DOI:10.1016/0734-189X(85)90125-2.

[11] P. Iliev, P. Tzvetkov, G. Petrov. Multidimensional dynamic scene analysis using 3D image histogram and entropy sequences analysis (bulgarian). *Int J Comp* **6**(1):35–43, 2007.

[12] A. Zhyrova, D. Stys, P. Cisar. Information entropy approach as a method of analysing Belousov-Zhabotinsky reaction wave formation. *Chem Listy* **107**(Suppl. 3):S341–S342, 2013.

[13] R. Rychtáriková. Clustering of multi-image sets using rényi information entropy. In F. Ortuño, I. Rojas (eds.), *IWBBIO 2016, Lect Notes Bioinf*, vol. 9656, pp. 517–526. 2016. DOI:10.1007/978-3-319-31744-1_46.

[14] R. Rychtáriková, T. Náhlík, K. Shi, et al. Super-resolved 3-D imaging of live cell's organelles from bright-field photon transmission micrographs. *Ultramicroscopy* **179**:1–14, 2017. DOI:10.1016/j.ultramic.2017.03.018.

[15] A. Zhyrova, D. Štys. Construction of the phenomenological model of Belousov-Zhabotinsky reaction state. *Int J Comp Math* **91**(1):4–13, 2014. DOI:10.1080/00207160.2013.766332.

[16] D. Štys, J. Urban, R. Rychtáriková, et al. Measurement in biological systems from the self-organisation point of view. In F. Ortuño, I. Rojas (eds.), *IWBBIO 2015, Lect Notes Bioinf*, vol. 9044, pp. 431–443. 2015. DOI:10.1007/978-3-319-16480-9_43.

[17] R. Rychtáriková, J. Korbel, P. Macháček, et al. Point information gain and multidimensional data analysis. *Entropy* **18**(10):372, 2016. DOI:10.3390/e18100372.

[18] T. Náhlík, J. Urban, P. Císař, et al. Entropy based approximation to cell monolayer development. In A. Jobbággy (ed.), *5th IFMBE, IFMBE Proc.*, vol. 37, pp. 563–566. 2011. DOI:10.1007/978-3-642-23508-5_146.

[19] T. Náhlík, D. Štys. Microscope point spread function, focus and calculation of optimal microscope set-up. *Int J Comp Math* **91**(2):221–232, 2014. doi:10.1080/00207160.2013.851379.

[20] J. Urban, J. Vanek, D. Stys. Preprocessing of microscopy images via shannon's entropy. PRIP 2009, Belarusian State University, Belarussia. *Proc PRIP 2009* pp. 183–187, 2009.

[21] J. Urban, J. Vaněk. Preprocessing of microscopy images via Shannon's entropy on GPU. GraVisMa 2009, Pilsen, Czechia. *Workshop Proc* pp. 48–51, 2009.

[22] J. Urban, J. Vaněk, D. Stys. Preprocessing of microscopy images via Shannon's entropy, ÖAGM/AAPR Workshop, Graz, Austria. *ÖAGM/AAPR Workshop* pp. 48–51, 2011.

[23] T. Boublík. *Statistická termodynamika (Czech). Statistical Thermodynamics*. Academia, Prague, Czechia, 1996.

[24] P. Jizba, T. Arimitsu. The world according to Rényi: thermodynamics of multifractal systems. *Ann Phys* **312**(1):17–59, 2004. doi:10.1016/j.aop.2004.01.002.

[25] C. E. Shannon. A mathematical theory of communication. *Bell Syst Techn J* **27**(3):379–423, 1948. doi:10.1002/j.1538-7305.1948.tb01338.x.

[26] C. E. Shannon. A mathematical theory of communication. *Bell Syst Techn J* **27**(4):623–656, 1948. doi:10.1002/j.1538-7305.1948.tb00917.x.

[27] O. Demirkaya, M. H. Asyali, P. K. Sahoo. *Image processing with Matlab: Applications in medicine and biology*. CRC Press, 2009.

[28] M. Nixon, A. Aguado. *Feature extraction & image processing*. Academic Press, 2002.

[29] S. Kullback, R. A. Leibler. On information and sufficiency. *Ann Math Stat* **22**(1):79–86, 1951. doi:10.1214/aoms/1177729694.

[30] General-purpose computation using gpus. `www.gpgpu.org`.